Preparation and Characterization of Epoxy/Kaolinite Nanocomposites

Xinnian Xia, Xiaoliang Zeng, Jia Liu, Weijian Xu

Institute of Polymer Research, College of Chemistry and Chemical Engineering, Hunan University, Changsha 410082, People's Republic of China

Received 26 September 2009; accepted 10 March 2010
DOI 10.1002/app.32421
Published online 22 June 2010 in Wiley InterScience (www.interscience.wiley.com).

ABSTRACT: Epoxy/kaolinite nanocomposites were prepared by adding the organically modified layered kaolinite to an epoxy resin [biphenyl phenol novolac epoxy resin (BPNE)] with 4,4′-diamino biphenyl sulfone (DDS) as a curing agent. The dispersion state of the kaolinite within crosslinked epoxy-resin matrix was examined by X-ray diffraction (XRD) and transmission electron micrograph (TEM). The effects of kaolinite on thermal properties were investigated and discussed by differential scanning calorimetry (DSC) and thermogravimetric analysis (TGA). Experimental results show that BPNE/kaolinite nanocomposites exhibit improved thermal than pure BPNE. When the kaolinite content is 5 wt %, the BPNE/kaolinite nanocomposites show the best thermal properties. These results indicate that nanocomposition is an efficient and convenient method to improve the thermal properties of BPNE. © 2010 Wiley Periodicals, Inc. J Appl Polym Sci 118: 2461–2466, 2010

Key words: nanocomposites; epoxy resins; kaolinite; thermal properties

INTRODUCTION

Epoxy resins are extensively used in many industry field as coatings, adhesives, insulating and substrate materials due to their good thermal and dimensional stability, excellent chemical and corrosion resistance; high tensile strength and modulus; good adhesion to many substrates.[1] The common epoxy resin systems, however, cannot satisfy some applications, which require high thermal resistance. Therefore, to remedy this, many studies have been reported to improve the thermal properties of epoxy resins.[2–4] One of the most well known methods is the synthesis of layered inorganic-polymer nanocomposites based on intercalation of polymer into layered inorganic materials. Because of the large contact area between the polymer and clay through a nanoscaled hybrid, nanocomposites generally exhibit improvements in properties of polymeric materials even at a small amount of clay (1–10%).[5] Among the nanocomposites, the most widely utilized clay is the montmorillonite for its large cation exchange capacity.[6–13]

Kaolinite is one of the most ubiquitous clay minerals in the earth, mostly found in soils, sediments and sedimentary rocks and is one of the most important raw materials for industrial uses. Despite its great abundance, high crystallinity, and high purity when compared with other mineral clays, only a limited number of kaolinite intercalation with organic polymers has been reported[14–19] as the low reactivity of kaolinite for intercalation, especially intercalation with epoxy resin.

In this study, inorganic kaolinite was modified by dimethyl sulfoxide (DMSO), and then epoxy/kaolinite nanocomposites were prepared via curing with DDS. The microstructural analysis of nanocomposites was examined by XRD and TEM techniques. The thermal degradation kinetics and the thermal stability behavior were evaluated by DSC and TGA.

EXPERIMENTAL

Materials

The kaolinite used was obtained from China-Kaolin Company, China. DMSO, DDS, methanol and other solvents were of reagent grade or better and procured from Shanghai Chemicals, China. The BPNE [epoxide equivalent weight (EEW) = 263] was synthesized according to the literature.[20] The theoretical molecular structure of this epoxy resin has the following form given in Scheme 1.

Preparation of kaolinite-DMSO

A mixture of kaolinite (10 g), DMSO (100 mL), and pure water (10 g) were added in a three-necked flask

Correspondence to: W. Xu (weijianxu_59@163.com).
Contract grant sponsor: Planned Science and Technology Project of Hunan province; contract grant number: 2008FJ3116.

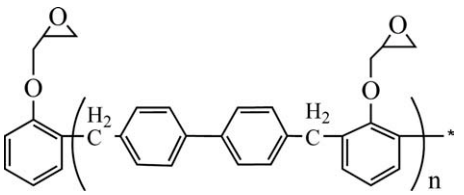

Scheme 1 Theoretical molecular structure of BPNE (n = 0–3).

fitted with a condenser and mechanical stirrer at 80°C and the contents were stirred at this temperature for 72 h. After the reaction was finished, the suspending system was filtered and washed by ethanol three times in order to get rid of the excess DMSO and distilled water. The washed kaolinite was dried at 50°C under vacuum for 24 h. IR (KBr, cm^{-1}): 3540 and 3507 cm^{-1} (—OH), 3022 and 2937 cm^{-1} (C—H stretching).

Preparation of BPNE/kaolinite nanocomposites

The epoxy resin (BPNE) was mixed with the organophilic kaolinite, in varied proportions of 0, 3.0, 5.0, 7.0, and 10.0 wt % based on the amount of the BPNE (as given in Table I). The mixture was then placed in a round-bottomed flask, heated until 80°C and mechanically stirred for 2 h at 80°C. After mixing up of organoclay and the resin thoroughly, DDS curing agent was added according to their stoichiometric ratio. The well-mixed system was poured into a mold. The resin was then cured at 80°C/1 h, 150°C/2 h, 180°C/2 h, and 200°C/2 h. The cured resin was cooled naturally. The nanocomposite synthesized was characterized using several techniques.

Characterizations

The Fourier transform infrared spectroscopy (FTIR) measurements of the organo-kaolinite dispersed in potassium bromide discs were carried out with a WQF-410.The wavelength of spectrum was from 4000 to 400 cm^{-1} with a resolution of 4 cm^{-1}.

XRD was performed on a Bruker D8 instrument. The analyses were carried out with a scanning rate of 2°/min with Cu κ_α radiation (λ = 1.5406 Å) at a generator voltage of 40 kV and current of 100 mA. The range of the diffraction angle was 2° to 70° (2θ).

TABLE I
Composition of the Nanocomposites

Sample number	Epoxy (g)	DDS (g)	Kaolinite (g)
EP-K0	100	17.4	0
EP-K1	100	17.4	3
EP-K2	100	17.4	5
EP-K3	100	17.4	7
EP-K4	100	17.4	10

The positions of the peak maximum and corresponding d-spacing were computed from the Bragg's diffraction equation: $\sin\theta = n\lambda/2d$, where n is the order of reflection, λ is the wavelength of radiation, and d is the interlamellar spacing.

TEM was conducted in JEOL-1230 instrument at an accelerating voltage of 100 kV. Thin sections (70 nm) of the specimen were obtained by microtome with diamond knife for TEM analysis. All the images were taken in bright field imaging mode.

DSC was employed to record the glass transition temperature (T_g) values of neat epoxy and the nanocomposites. The DSC thermograms were recorded with a thermal analysis (TA) at a heating rate of 10°C/min under nitrogen atmosphere. Thermogravimetric analysis (TGA) was performed by a STA-449C Thermo gravimetric analyzer at a heating rate of 10°C/min under nitrogen atmosphere.

RESULTS AND DISCUSSION

Characterization of kaolinite-DMSO

Figure 1 shows the FTIR spectrum of raw kaolinite (a) and kaolinite-DMSO (b). As can be seen from Figure 1(b), the absorption peak of hydroxyl (—OH) of raw kaolinite at 3694 cm^{-1} has completely disappeared. The new absorption peaks of hydroxyl (—OH) of kaolinite-DMSO at 3540 and 3507 cm^{-1} can be observed. The absorption bands at 3022 and 2937 cm^{-1} belong to the C—H stretching frequencies of DMSO.

Figure 2 exhibits the XRD patterns of raw kaolinite and kaolinite-DMSO. As the figure exhibited, the raw kaolinite has a d(001) spacing of 0.72 nm. The d(001) spacing of kaolinite-DMSO increased to 1.13 nm [Fig. 2(b)] due to intercalation of DMSO with

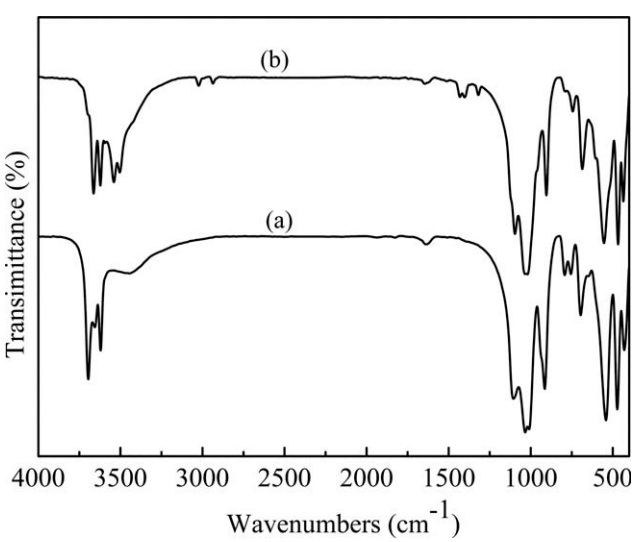

Figure 1 FTIR spectra of raw kaolinite (a) and kaolinite-DMSO (b).

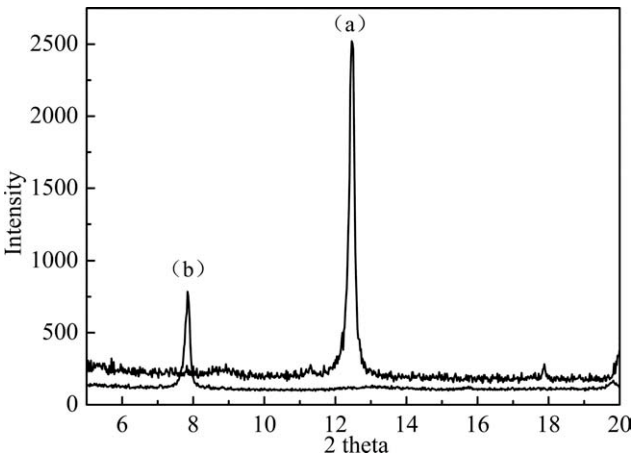

Figure 2 X-ray diffractions of raw kaolinite (a) and kaolinite-DMSO (b).

kaolinite. These molecules remain absorbed during the drying step, keeping the platelets away from collapsing due to interlayer hydrogen bonding. These results confirm that intercalation between kaolinite and DMSO had taken place.

Morphology

XRD and TEM were used to characterize the morphology of nanocomposites. The XRD patterns of the epoxy resin nanocomposites are shown in Figure 3. It is observed that the epoxy nanocomposite (up to 5 wt % of kaolinite) do not show any sharp diffraction peaks in the XRD pattern. This indicates that the clay has moved from intercalated region to exfoliated region. The interlayer spacing distance of the clay has been increased above 75 nm in which Bragg's law does not obey. When the kaolinite loading is higher than 5%, however, the $d(001)$ reflection of kaolinite is observed ($2\theta = 12.24$), indicating the aggregated kaolinite is in the epoxy resin matrix.

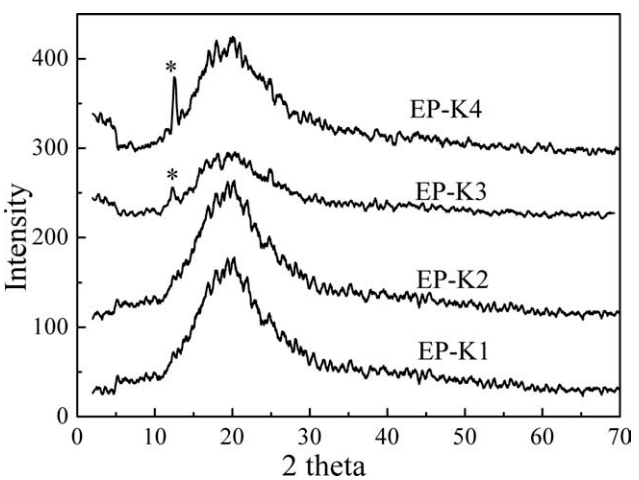

Figure 3 XRD patterns of epoxy resin nanocomposites.

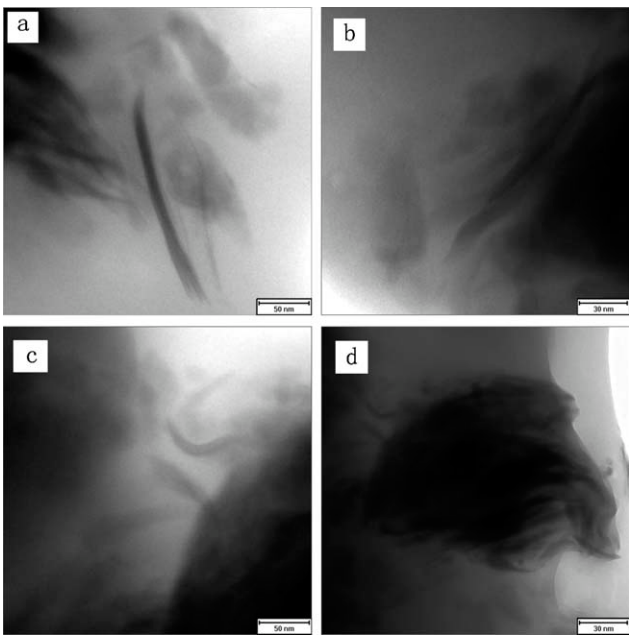

Figure 4 TEM micrographs of epoxy nanocomposites: (a) EP-K1, (b) EP-K2, (c) EP-K3, (d) EP-K4.

This XRD data suggests different kaolinite loadings lead to various degree of exfoliation.

To investigate in detail the interaction between kaolinite and BPNE, TEM images of BPNE nanocomposites are shown in Figure 4. The dark lines are the clay layers dispersed in the epoxy resin matrix. It reveals that the prepared nanocomposites are in the fully exfoliated state [Fig. 4(a,b)]. In Figure 4(c,d), kaolinite aggregates can be detected. The dispersion of kaolinite decreases with the increase of kaolinite concentration. It suggests that the exfoliation would be constrained if more kaolinite were added.

DSC analysis

The glass transitions (T_g) of neat epoxy resin and nanocomposites were measured by DSC and reported in Figure 5. The T_g values are listed in Table II. As the results in Table II show, with increasing the kaolinite contents, the T_g of nanocomposites tends to move to higher values relative to the T_g of the neat system (165.2°C). The epoxy resin gives the highest T_g at 5% loading of kaolinite. After that it starts to decrease.

According to the coupling model theory suggested by Roland and Ngai,[21] the segmental motion of polymers below T_g is a cooperative process and has to overcome the resistance from the surrounding segments in order to accomplish the transformation between configurations. As more segments are restricted by the presence of kaolinite, the activation threshold for the motion of some segments becomes higher. As a consequence, epoxy/kaolinite nanocomposites have

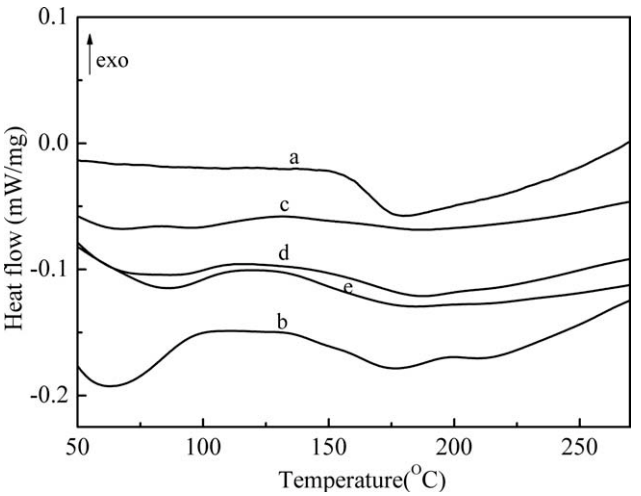

Figure 5 DSC thermograms of epoxy nanocomposites: (a) EP-K0, (b) EP-K1, (c) EP-K2, (d) EP-K3, (e) EP-K4.

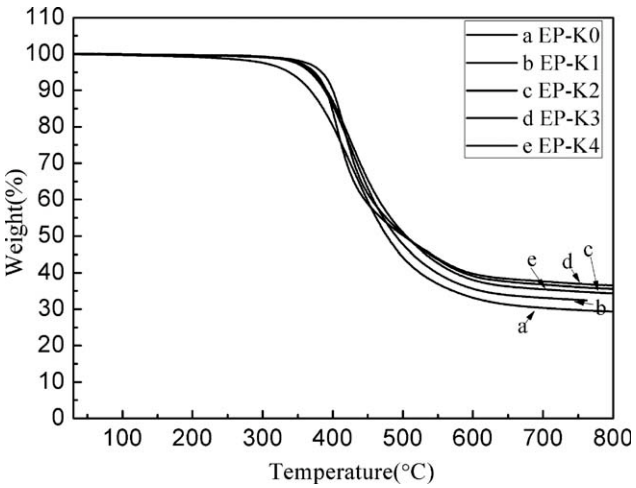

Figure 6 TGA curves under nitrogen flow of neat BPNE and BPNE/kaolinite nanocomposites with different clay contents.

exhibited a higher T_g than the corresponding neat resin system. With the increase of the loading, the T_g increases and optimum conditions were achieved at 5% by weight loading. However, as the content is over 5 wt %, the T_g decrease. The cause for this is certainly the lack of uniform dispersion. The agglomerated particles decrease the crosslinking and ultimately the T_g.

Thermogravimetric analysis

The thermal stability of the systems was evaluated by means of TGA analyses. Figure 6 represents TGA curves as a function of weight losses of nanocomposites. Table III contains parameters characterizing the thermal degradation such as $T_{d5\%}$, $T_{d10\%}$ char yield. From the TGA data, it is clear that the $T_{d5\%}$, $T_{d10\%}$ and char yield of the nanocomposite shifted toward the higher temperature as the amount of kaolinite increases. Furthermore, it is noted that the $T_{d5\%}$ and $T_{d10\%}$ reach a maximum value at 5% of kaolinite, which is higher by $\sim$ 21.8°C and 13.2°C than the $T_{d5\%}$ and $T_{d10\%}$ of the neat epoxy resin, respectively. However, with 7% kaolinite, the char yield at 800°C goes through a maximum, with values $\sim$ 7.2% higher in relation to the unmodified resin.

The thermal stability increase have been observed in other organic–inorganic nanocomposites[10,22–25] and are generally attributed to the effects such as a decrease in permeability due to the so-called "tortuous path" effect of the filler.[26,27] The clay, together with the solid degradation products, lead to a dense coating. This dense coating delays the permeation of oxygen and the escape of volatile degradation products and char formation. The effect of kaolinite loading on thermal stability of epoxy resin nanocomposites can be explained by the structure evolution as the kaolinite loading change. When the kaolinite is relatively low (below 5%), the nanocomposite develops an exfoliation dominant structure. The retardant effects of the exfoliated platelet to heat and oxygen in the epoxy matrix is strengthened when the kaolinite loading increases since the number of the exfoliated platelets increases with kaolinite loading. When the kaolinite loading increases further, the number of exfoliated silicate platelet decreases. As a consequence, the thermal stability decreases when the kaolinite loading is higher than 5%. As the tactoids still show the retardant effects to heat and oxygen, the thermal stability of the sample with exfoliated/intercalated structure is still higher than that of the neat epoxy resin.

TABLE II
T_g of Neat Epoxy Resin and Nanocomposites

Sample number	T_g (°C)
EP-K0	165.2
EP-K1	166.4
EP-K2	171.2
EP-K3	167.8
EP-K4	167.2

TABLE III
Thermal Stability Parameters Calculated from the TGA curves

Sample number	$T_{d5\%}$ (°C)[a]	$T_{d10\%}$ (°C)[b]	$W_{800°C}$ (%)[c]
EP-K0	363.1	386.8	29.37
EP-K1	367.9	388.4	32.17
EP-K2	384.9	400.1	35.6
EP-K3	373.8	390.5	36.54
EP-K4	369.7	391.2	34.35

[a] Temperature at which 5% of the mass is volatilized.
[b] Temperature at which 10% of the mass is volatilized.
[c] Char yield at 800°C.

Thermal degradation kinetics

To evaluate the thermal stability more detailed, nonisothermal thermal degradation kinetics were calculated. For an *n*-order reaction, the reaction rate can express as:

$$\frac{d\alpha}{dt} = k(1-\alpha)^n \quad (1)$$

Where, α is the apparent conversion, k is the rate constant, n is the reaction order.

In dynamic mode, the mathematical representation takes the following form:

$$\frac{d\alpha}{dt} = \frac{A}{\phi}\exp\left(\frac{-E_\alpha}{RT}\right)(1-\alpha)^n \quad (2)$$

where, E_α is the apparent activation energy, ϕ is the heating rate and A is the Arrhenius frequency factor.

Different kinetics expressions could be obtained by integrating the above equation with different approximation treatments. Among those kinetics equations, the Coats-Redfern equation[28] is one of the well-known models. It is mathematically represented as:

$$\ln\left[\frac{g(\alpha)}{T^2}\right] = \ln\left[\frac{\frac{AR}{E_\alpha\phi}}{1-\frac{2RT}{E_\alpha}}\right] - \frac{E_\alpha}{RT} \quad (3)$$

where

$$g(\alpha) = \frac{1-(1-\alpha)^{1-n}}{1-\alpha} \quad (4)$$

If the order is equal to 1,

$$g(\alpha) = -\ln(1-\alpha) \quad (5)$$

$$\ln\left[\frac{-\ln(1-\alpha)}{T^2}\right] = \ln\left[\frac{\frac{AR}{E_\alpha\phi}}{1-\frac{2RT}{E_\alpha}}\right] - \frac{E_\alpha}{RT} \quad (6)$$

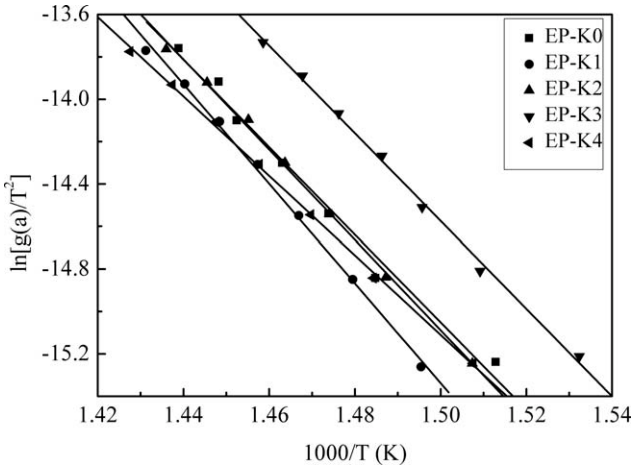

Figure 7 Kinetics of thermal decomposition of epoxy nanocomposites by Coats–Redfern equation.

TABLE IV
Kinetic Data of Epoxy Nanocomposites by Coats–Redfern Equation

Sample number	E_α (kJ/mol)	R (linear correlation coefficients)
EP-K0	164.1	0.993
EP-K1	177.0	0.998
EP-K2	183.2	0.998
EP-K3	173.4	0.998
EP-K4	157.8	0.999

For the decomposition of thermosets, the mechanism of random scission of molecules dominates. Therefore, the decomposition could be treated as one order reaction. Making fitted linear regression lines, high correlation coefficients ($R > 0.99$) were obtained for all of the linear regression curves of ln $[-\ln(1-\alpha)/T^2]$ versus $1000/T$. For each experimental curve, the slope (E_α) of the corresponding plot was calculated. Figure 7 shows the Coats-Redfern curve treated with one order reaction. The apparent activation energies are summarized in Table IV.

As can be seen from the Table IV, the activation energy is a function of kaolinite loading. The activation energy reaches a maximum at 5% kaolinite loading. The changes in activation energy of the nanocomposites are consistent with the changes of $T_{d5\%}$ and $T_{d10\%}$. This trend of E_α is also attributed to the structure evolution as the kaolinite loading increases.

CONCLUSIONS

In this study, the epoxy/kaolinite nanocomposites were prepared by dispersing kaolinite pretreated by DMSO into the BPNE/DDS cured system. From TEM and XRD results, the aggregation phenomena of kaolinite nanoparticles became more significant as the kaolinite content increased. TGA and DSC analysis indicated that the thermal stability of epoxy/kaolinite nanocomposites increased with the kaolinite content increased from 0% to 10%. Among various contents of kaolinite in the nanocomposites, epoxy/5% kaolinite nanocomposite had the maximum $T_{d5\%}$, $T_{d10\%}$, and T_g. Furthermore, the nonisothermal thermal degradation kinetics were calculated. The maximal value of activation energy is 183.2 kJ/mol with the addition of 5% kaolinite. The results obtained in this work allow the conclusion that the kaolinite infusion improves the thermal properties of the epoxy resin.

References

1. Park, S. J.; Jin, F. L.; Lee, J. R. Mater Sci Eng A 2004, 373, 109.
2. Pan, G.; Du, Z.; Zhang, C.; Li, C.; Yang, X.; Li, H. Polymer 2007, 48, 3686.
3. Xu, K.; Chen, M.; Zhang, K.; Hu, J. Polymer 2004, 45, 1133.

4. Zhang, X. H.; Chen, S.; Min, Y. Q.; Qi, G. R. Polymer 2006, 47, 1785.
5. Pavlidou, S.; Papaspyrides, C. D. Prog Polym Sci 2008, 33, 1119.
6. Ren, J.; Yu, T.; Li, H.; Ren, T. B.; Yang, S. Polym Compos 2008, 29, 1145.
7. Tsai, T. Y.; Lu, S. T.; C Li, H.; Huang, C. J.; Liu, J. X.; Chen, L. C. Polym Compos 2008, 29, 1098.
8. Dai, C. F.; Li, P. R.; Yeh, J. M. Eur Polym J 2008, 44, 2439.
9. Kowalczyk, K.; Spychaj, T. Prog Org Coat 2008, 62, 425.
10. Lakshmi, A. S.; Narmadha, B.; Redd, B. S. R. Polym Degrad Stab 2008, 93, 201.
11. Musto, P.; Abbate, M.; Ragosta, G.; Scarinzi, G. Polymer 2007, 48, 3703.
12. Tan, H. L.; Han, J.; Ma, G. P.; Xiao, M.; Nie, J. Polym Degrad Stab 2008, 93, 369.
13. Miyagawa, H.; Rich, M. J.; Drzal, L. T. Polym Compos 2005, 26, 42.
14. Eristi, C.; Yavuz, M.; Yilmaz, H.; Sari, B.; Unal, H. I. J Macromol Sci Part A: Pure Appl Chem 2007, 44, 759.
15. Wan, T.; Wang, X. Q.; Yuan, Y.; He, W. Q. J Appl Polym Sci 2006, 102, 2875.
16. Bahramian, A. R.; Kokabi, M.; Famili, M. H. N.; Beheshty, M. H. J Hazard Mater 2008, 150, 136.
17. Elboklt, A.; Detellier, C. Can J Chem 2009, 87, 272.
18. Essawy, H. A.; Youssef, A. M.; Abdel-Hakim, A. A.; Rabie, A. M. Polym Plast Eng 2009, 48, 177.
19. Li, Y. F.; Zhang, B.; Pan, X. B. Compos Sci Technol 2008, 68, 1954.
20. Jibiki, H.; Honma, T.; Noday, Y.; Okazakik, K.; Kashima, M. U.S. Pat. 5,612,442 (1997).
21. Roland, C. M.; Ngai, K. L. Macromolecules 1991, 24, 5315.
22. Bae, S. B.; Kim, C. K.; Kim, K.; Clung, I. J. Eur Polym J 2008, 44, 3385.
23. Mencel, K.; Kelar, K.; Jurkowski, B. I. Polimery 2009, 54, 361.
24. Zhang, Y.; Liu, W.; Han, W.; Guo, W. H.; Wu, C. F. Polym Compos 2009, 30, 38.
25. Cabeda, L.; Gimenez, E.; Lagaron, J. M.; Gavara, R.; Jsaura, J. Polymer 2004, 45, 5233.
26. Mclauchlin, A. R.; Thomas, N. L. Polym Degrad Stab 2009, 94, 868.
27. Guo, B. C.; Ha, D. M.; Cai, C. G. Eur Polym J 2004, 40, 1743.
28. Kahrizsangi, R. E.; Abbasi, M. H. Trans Nonferrous Met Soc China 2008, 18, 217.